1-1-2013

Correlation of embryonic skeletal muscle myotube physical characteristics with contractile force generation on an atomic force microscope-based bio-microelectromechanical systems device

K. L. Pirozzi
University of Central Florida

C. J. Long
University of Central Florida

C. W. McAleer
University of Central Florida

A. S. T. Smith
University of Central Florida

J. J. Hickman
University of Central Florida

Correlation of embryonic skeletal muscle myotube physical characteristics with contractile force generation on an atomic force microscope-based bio-microelectromechanical systems device

Cite as: Appl. Phys. Lett. **103**, 083108 (2013); https://doi.org/10.1063/1.4817939
Submitted: 07 June 2013 . Accepted: 23 July 2013 . Published Online: 20 August 2013

K. L. Pirozzi, C. J. Long, C. W. McAleer, A. S. T. Smith, and J. J. Hickman

Correlation of embryonic skeletal muscle myotube physical characteristics with contractile force generation on an atomic force microscope-based bio-microelectromechanical systems device

K. L. Pirozzi,[a] C. J. Long,[a] C. W. McAleer, A. S. T. Smith, and J. J. Hickman[b]
NanoScience Technology Center, University of Central Florida, 12424 Research Parkway, Orlando, Florida 32826, USA

(Received 7 June 2013; accepted 23 July 2013; published online 20 August 2013)

Rigorous analysis of muscle function in *in vitro* systems is needed for both acute and chronic biomedical applications. Forces generated by skeletal myotubes on bio-microelectromechanical cantilevers were calculated using a modified version of Stoney's thin-film equation and finite element analysis (FEA), then analyzed for regression to physical parameters. The Stoney's equation results closely matched the more intensive FEA and the force correlated to cross-sectional area (CSA). Normalizing force to measured CSA significantly improved the statistical sensitivity and now allows for close comparison of *in vitro* data to *in vivo* measurements for applications in exercise physiology, robotics, and modeling neuromuscular diseases. © *2013 AIP Publishing LLC*. [http://dx.doi.org/10.1063/1.4817939]

Recent advances in skeletal muscle bioengineering have allowed for the development of *in vitro* models capable of accurately measuring and temporally controlling the contractile function of cultured muscle myotubes, the smallest complete functional component of skeletal muscle.[1–5] However, most of these methodologies rely on the investigation of dense arrays of myotubes encased in 3D hydrogels.[1,4,5] The use of such systems therefore prevents the study of the functional responses of individual myotubes to physical, chemical, or pathological challenges. An *in vitro* system that can reproduce the primary metrics obtained for *in vivo* exercise physiology could vastly improve research in this important area of human health.

Simple micro-scale cantilevers have been used extensively for a variety of microelectromechanical system (MEMS) devices including resonators, energy harvesting devices, and an array of actuators and sensors.[6–9] However, complete understanding and widespread use of these systems were not achieved until modeling of their function in complex environments was performed.[10,11] The simplicity of the geometry and wide use of cantilevers in MEMS devices provides a system with well-characterized mechanics as a platform to incorporate biological components for medical and physiological research. The same underlying physics and simulation based modeling tools used to understand other cantilever-based devices can now be applied to bio-microelectromechanical (bioMEMS) cantilever systems to perform micro-scale force measurements on biological tissues that have previously only been performed on the macro-scale or with human or animal subjects.

A bioMEMS based on silicon cantilevers has been used to measure contraction characteristics of single myotubes.[3,12] Modeling this system would allow investigators to normalize force outputs based on physical parameters for both acute and chronic studies, and thereby achieve more precise data regarding the effects of chemical or pathological challenges to muscle fibers *in vitro*, applications in exercise physiology or for use as model systems to design the next generation of robotic systems. *In vivo*, muscle force generation has been shown to correlate to muscle cross-sectional area (CSA) above other possible predictors,[13–15] and studies of muscle tissue constructs grown *in vitro* have normalized force to CSA.[1,4,16,17] However, detailed analysis of correlation of force generation of *in vitro*-grown skeletal muscle to morphological parameters is lacking. Specifically, studies investigating morphological effects on force generation of single myotubes are absent from the literature.

Another limit to the analytical power of the previous studies using this cantilever system was the reliance on treating each of the myotubes analyzed as a uniform film of standard thickness and width across the cantilever. This assumption permitted calculation of myotube stress in response to contraction using a modified version of Stoney's equation, which was established to measure stress in a thin film.[18] The thin-film approximation is very simple to apply for data analysis, but a finite element analysis (FEA) approach to modeling myotubes is more rigorous due to more detailed mechanical calculations of the internal forces in the cell. Given the increase in computational complexity that FEA entails, a direct comparison to the Stoney's equation approach, in terms of measuring myotube contraction on cantilever bioMEMS device, would provide valuable information to researchers for selecting the most appropriate method for each specific application, particularly in the use of high throughput systems in which the FEA approach would be cumbersome. However, demonstrating FEA's usefulness in the analysis of the system enables a much deeper understanding of the physics of muscle function and its integration with MEMS devices.

Silicon chips containing arrays of cantilevers 750 μm long, 100 μm wide, and 4 μm thick were produced from silicon-on-insulator (SOI) wafers using standard fabrication

[a]K. L. Pirozzi and C. J. Long contributed equally to this work.
[b]Author to whom correspondence should be addressed. Electronic mail: jhickman@mail.ucf.edu. Telephone: 407-823-1925. Fax: 407-882-2819

techniques, as detailed previously.[3] To produce a defined surface chemistry supportive of muscle progenitor cell attachment, growth, and myotube formation, the silicon cantilevers were silanized with (3-trimethoxy propyl)diethylenetriamine (DETA), a silane possessing the amine-containing moiety, diethylenetriamine.[3]

Skeletal muscle was dissected from the hind limbs of fetal rat embryos (18 days *in utero*) following a previously established protocol.[19] The skeletal muscle was plated on the bioMEMS cantilever device at a density of 2000 cells/mm^2 and allowed to proliferate for 4 days in a defined serum-free medium.[12,20] After 4 days in culture, the medium was completely removed and replaced with NbActiv4 (Brain Bits LLC) to induce myotube formation; a one half medium change was performed with NbActiv4 every 3–4 days subsequently. Following 12–14 days *in vitro* (DIV), the cultures were analyzed for contractile stress according to a previously established protocol.[3] Briefly, the myotubes were stimulated under an electric field with 40 ms pulse-widths at a rate of 1 Hz in order to induce contraction of the myotubes on the cantilevers. Each cantilever's response to myotube contraction was measured by monitoring the deflection of a laser beam focused on the bottom of the cantilever tip. Deflections of the light beam were measured using a photo-detector and recorded in real time by a computer running Axoscope 10.0 software. The noise in the measurement signal was typically less than 2% of the peak signal from myotube contraction. The temporally dependent deflection of each cantilever tip was calculated from the laser displacement data and constants related to the system setup. The data were collected utilizing 12 independent myotubes from 3 cultures.

Cantilevers were prepared for immunocytochemical analysis as previously described.[21] Cells were incubated overnight with a primary antibody against Myosin Heavy Chain (A4.1025) (Developmental Studies Hybridoma Bank) diluted (1:10) in a pH buffered solution. Alexa Fluor 594 conjugated phalloidin (Invitrogen a12381) was added to this solution (1:40 dilution) in order to facilitate Actin filament visualization. Cells were then incubated with the appropriate secondary antibody for 2 h in the same pH buffered solution and evaluated using confocal microscopy. A Z-stack analysis was performed taking 1 μm slices from the top of the myotube to the base. The individual slices were collated, using ImageJ software,[22] to create a three-dimensional rendering of the myotube. From the three-dimensional rendering, the length, average width, and average thickness of each myotube were determined.

The Stoney's equation approach was used to calculate the compressive stress generated by the myotube from the voltage output of the photo-detector (Volts). The equations and methods described previously[3] were modified to account for the measured width of the myotube instead of assuming the myotube filled the entire width of the cantilever. Equations (1) and (2) are restated versions for cantilever tip deflection (δ) and stress produced by the myotube, assuming a uniform thick film the full width of the cantilever (σ_c). The system parameters used in these equations are the system-specific coefficient relating voltage to laser position on the photo-detector ($C_{detector}$), the angle of the laser and detector relative to the plane of the cantilever (θ), the path length of the laser from the cantilever tip to the detector (P), the elastic modulus of silicon (E_{Si}), the thicknesses of the cantilever (t_{Si}) and myotube (t_f), Poisson's ratio of silicon (v_{Si}), cantilever length (L), and the widths of the cantilever (w_{Si}) and myotube ($w_{myotube}$)

$$\delta = \frac{2L}{3}\tan\left[\frac{\theta}{2} - \frac{1}{2}\arctan\left(\tan\theta - \frac{Voltage}{C_{detector} \times P \times \cos\theta}\right)\right]. \quad (1)$$

In Eq. (2), the myotube is approximated as a uniform film. Therefore, the force in the myotube is equal to the force in the film, leading to Eq. (3) by equating the calculation of force from stress and CSA. To determine stress in the myotube ($\sigma_{myotube}$), Eq. (3) can be rearranged to form Eq. (4)

$$\sigma_c = \frac{E_{Si}t_{Si}^3}{6t_f(1-v_{Si})(t_f+t_{Si})}\frac{3\delta}{2L^2} \times \frac{1}{1+\frac{t_f}{t_{Si}}}, \quad (2)$$

$$F_{myotube} = \sigma_c \times t_f \times w_{Si} = \sigma_{myotube} \times t_f \times w_{myotube}, \quad (3)$$

$$\sigma_{myotube} = \sigma_c \times (w_{Si}/w_{myotube}). \quad (4)$$

For the FEA approach, the cantilever geometry was drawn and meshed in NX 8.5 (Siemens PLM Software, Plano, TX) as a set of square elastic elements, with a fixed boundary condition at one end to produce a cantilevered geometry. For each myotube experimentally tested, the myotube was modeled as an ellipsoid on top of the cantilever in NX using the measured dimensions and positions acquired from confocal microscopy. In the FEA model, the myotube and cantilever beam were meshed with 3D square elements. The coincident nodes were merged, which allowed for the simulation of a fully adhered myotube to the cantilever beam. The stress in the myotube was determined using the FEA model by altering the force so that the deflection matched the value for deflection calculated from Eq. (1). The force in each myotube calculated from the Stoney's method was compared to the force calculated from the FEA for that myotube.

Multiple linear regression was applied to the force calculated from the Stoney's and FEA approaches to fit values to the physical dimensions of the myotubes and the interactions of these variables using a best fit approach to selecting predictive variables. Two of the variable interactions, width $\times$ thickness and width $\times$ thickness $\times$ length, were functionally equivalent to CSA and volume, respectively, differing by constant coefficients $\pi/4$ for the CSA and $\pi/6$ for the volume, assuming the myotubes were shaped as an ellipsoid. For determination of predictive variables from the regression analysis, the exact shape of the myotube was irrelevant as long as the volume was a product of a constant and the length $\times$ width $\times$ thickness interaction. The *in vitro* myotubes were observed to be approximately ellipsoidal, so this simple shape was used for calculating the CSA and volume for each myotube.

After selecting the best regression model, the force data were normalized to the model parameters, and the coefficient of variance (COV), the ratio of the standard deviation to the sample mean, was calculated. The COV was compared to the COV of the non-normalized data to determine the utility

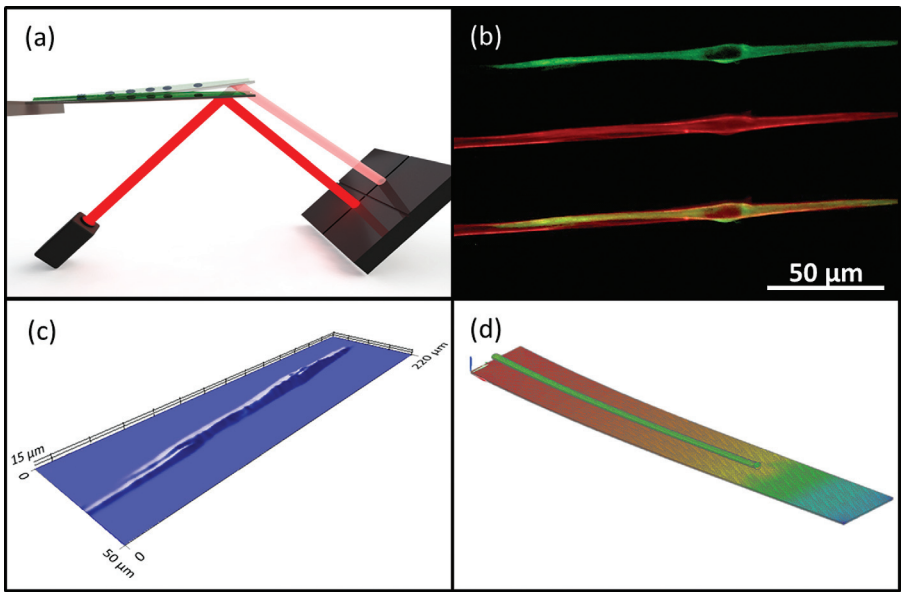

FIG. 1. Layout of the finite element analysis model and an example of myotube force estimation where stresses in the myotube and cantilever are displayed. (a) Schematic of measurement system configuration. (b) Immunocytochemistry of a single myotube showing myosin heavy chain (green) and actin (red) in individual channels and a merged composite. (c) Three dimensional representation produced from Z-stack of the actin images. (d) Example of FEA of a myotube with stress indicated with color.

of using the regression model for reducing variation for comparison among experimental treatment groups.

Bright field microscopy of the cultures, at 14 DIV, illustrated good morphology of the primary myotubes on the cantilevers. The myotube dimensions on the cantilevers as determined from confocal imaging ranged between the following values: length between 490 and 696 μm, width between 11.7 and 23.4 μm, and thickness between 7.9 and 13.0 μm. The force, as calculated from the modified Stoney's equation (Eqs. (1)–(3)), ranged from 38 nN to 256 nN, and the stress in the myotube (Eq. (4)) ranged from 350 to 1760 Pa. Using the FEA approach, the forces and stresses in the myotubes ranged from 25 to 181 nN and 168 to 1170 Pa, respectively. The layout of the system and examples of confocal imaging, 3D reconstruction of a myotube, and FEA are presented in Figure 1. Direct comparison of the force on each cantilever determined from the two methods revealed that the Stoney's equation approach matched the FEA approach in both trend and value, with a correlation coefficient (R) of 0.97. In terms of absolute force values, the forces from Stoney's equation differed from the FEA by a factor of roughly 1.4. Considering the vast differences in the mathematics involved between the two methods, these two approaches yielded force values that were well matched for simple systems. Figure 2 graphically indicates the differences between the forces calculated by the Stoney's equation approach and the FEA approach.

Regression analysis of the force in the myotube as calculated using the FEA approach determined that CSA as a sole predictor provided the best regression for force ($p = 0.02$), with a correlation coefficient (R-value) of 0.67 (R^2 of 0.45). The forces are graphed versus myotube CSA in Figure 3.

After normalizing the force data to the CSA, the coefficient of variance was greatly reduced versus the non-normalized data. The force normalized to CSA is by definition the stress in the myotube along the longitudinal axis. Normalizing the force to CSA decreased the COV by 14% and 19%, using the data from the Stoney's equation and FEA approaches, respectively. The signal-to-noise ratio—the inverse of the COV—changed more dramatically, with the

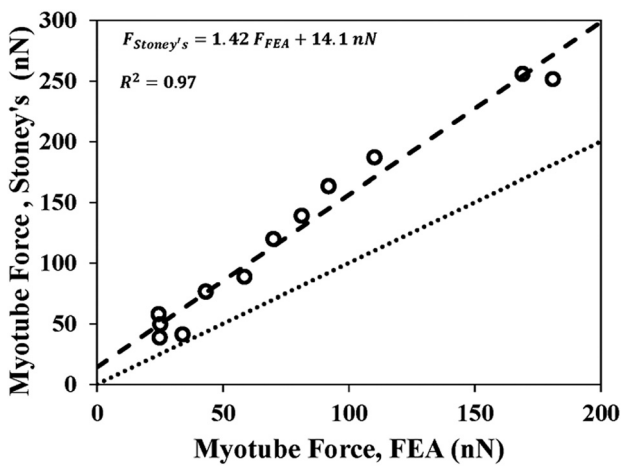

FIG. 2. The forces calculated from the Stoney's equation closely matched the forces calculated using finite element analysis ($R^2 = 0.97$, regression shown with dashed line). The deviation from the $y = x$ line (dotted line) for a given point indicates the variation in calculated forces from the two methods.

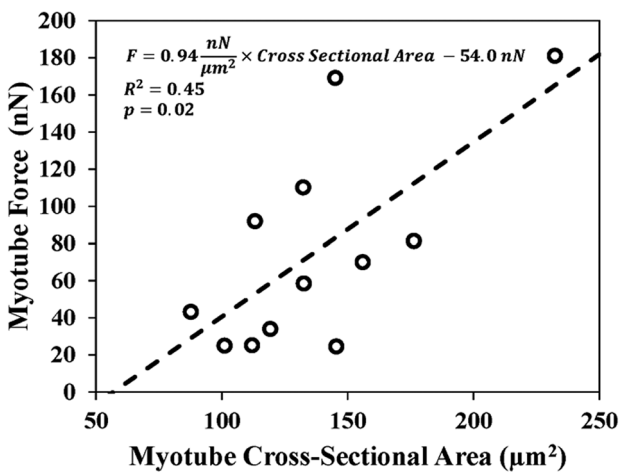

FIG. 3. Force generated by individual myotubes correlated with the myotube CSA ($R^2 = 0.45$), which was selected as the sole predictor for force by multiple regression analysis. Force values presented were calculated using the FEA approach.

area-normalized force exhibiting a 17% and 23% higher signal-to-noise ratios than the non-normalized force using the two methods. The use of cantilevers to determine stresses generated in a thin film on a cantilever beam is a well-established and understood field of physics, and we have shown it can be an adaptive solution to the technological need for stress measurement in biological tissues at the microscale.[23,24] The integration of muscle mechanics with silicon device mechanics and transduction now establish a controlled, predictable assay system, and the ability to model the hybrid system further allows a better understanding of the mechanisms for many applications in biotechnology. A direct correlation between myotube physical attributes and force production *in vitro*, as demonstrated here, is a significant finding, since it suggests the developed model closely parallels the functional characteristics of the native tissue, where muscle size, specifically cross-sectional area, has been shown to be directly linked to force production.[13–15] This bioMEMS device can now be transitioned into a system for the study of muscle physiology and muscle-related diseases for human drug discovery applications.

From a physiological perspective, the conclusion that myotube force generation scales with CSA validates that the *in vitro* data collected from the cantilever bioMEMS device matches the *in vivo* data trends.[13,25] The regression analysis sufficiently establishes that the CSA of a myotube is important in dictating its force generation capability. However, the fact that roughly 50% of the variation in the force values was not explained by the CSA indicates that this factor is not the sole determinant of myotube contractile force in this system. Reports correlating muscle strength to physical parameters *in vivo* demonstrated that the CSA is the best predictor of strength among the variables tested.[13–15] However, the *in vivo* strength data did not follow CSA exactly, with the R value roughly 0.5 ($R^2 \approx 0.3$) indicating substantial variation among human test subjects. The results from the *in vitro* system presented here demonstrated a considerable improvement to the correlation of force to CSA ($R = 0.7$). This system not only recapitulated the CSA dependence of muscle force generation, but also isolated the muscle component to remove inter-subject variation caused by other variables.

The finite element analysis of data collected from *in vitro* skeletal muscle myotubes on a cantilever validated the use of the Stoney's method approach for calculating force dynamics in this model. Regression analysis demonstrated that the force generated by a myotube is correlated to the myotube CSA. Normalizing the force to CSA to produce an accurate measure of stress and improved the coefficient of variance, allowing for 32% fewer samples required for statistical analysis of differences among means, or a 19% smaller difference among sample means that could be statistically detected using a given number of samples. Such improvements will be vital in studies where the difference in functional output between experimental groups is significant but small, and in cases where available tissue samples are limited so only relatively few experimental tests can be conducted. It should be noted that previous studies using this cantilever bioMEMS device reported stress, but the force data were not normalized to the area for each specific myotube.[3,12] Instead, system-wide values for myotube width and thickness were assumed for all myotubes. This assumption produces data that are not truly normalized to CSA, and the COV would mimic that of the non-normalized force data reported here.

In terms of the use of the computationally less intensive Stoney's equation instead of the finite element analysis for calculating force generation of the myotubes, both methods have advantages and disadvantages. The FEA approach is more time- and resource-intensive, but is more mechanically rigorous. This method is therefore most suitable for low-throughput applications in which small differences among means are expected. However, the increased mechanical rigor of the FEA resulted in only a small improvement in variability, indicating that Stoney's equation could be used in place of the FEA for many applications of this system. Thus, for biotechnology applications, Stoney's equation is a powerful method for improving throughput, considering that the assumptions and computational simplicity of this approach allow real-time output of force data once the dimensions of the myotube are known. In experiments where paired analysis is available, in which two or more treatments can be applied to the same myotubes and the data compared, the variation among myotubes is already accounted for by the paired format, and therefore the advantages of Stoney's equation become more prominent versus FEA. Normalizing functional output data to biophysical attributes, as has been performed in this study, facilitates closer comparisons between experimental groups, and improves the power of the statistical differences observed. Such improvements represent the means to greatly increase the relevance of this model to investigate skeletal muscle disease states since it allows observations made *in vitro* to be scaled, producing accurate predictions of *in vivo* responses. Furthermore, an ability to scale up observed *in vitro* responses based on physical parameters facilitates the tailoring of drug treatment dosages to an individual's muscle mass and may have significant applications in the development of personalized treatment regimes. Finally, improved predictions of *in vivo* responses from *in vitro* data are likely to accelerate future drug development and toxicology studies since greater power can be obtained in early pre-clinical screens.

This work was supported by NIH Grant Nos. R01NS050452 and R01EB009429. Special thanks to Mandy Esch for aiding microfabrication.

[1]R. G. Dennis, P. E. Kosnik II, M. E. Gilbert, and J. A. Faulkner, Am. J. Physiol.: Cell Physiol. **280**(2), C288 (2001).
[2]H. Vandenburgh, J. Shansky, F. Benesch-Lee, V. Barbata, J. Reid, L. Thorrez, R. Valentini, and G. Crawford, Muscle Nerve **37**(4), 438 (2008).
[3]K. Wilson, M. Das, K. J. Wahl, R. J. Colton, and J. Hickman, PLoS ONE **5**(6), 1 (2010).
[4]S. Hinds, W. Bian, R. G. Dennis, and N. Bursac, Biomaterials **32**(14), 3575 (2011).
[5]A. Khodabukus and K. Baar, Tissue Eng. **18**(5), 349 (2012).
[6]J. S. Burdess, B. J. Harris, D. Wood, R. J. Pitcher, and D. Glennie, J. Microelectromech. Syst. **6**(4), 322 (1997).
[7]T. Thundat, P. I. Oden, and R. J. Warmack, Microscale Thermophys. Eng. **1**(3), 185 (1997).
[8]R. Andosca, T. G. McDonald, V. Genova, S. Rosenberg, J. Keating, C. Benedixen, and J. R. Wu, Sens. Actuator, A **178**, 76 (2012).
[9]J. Fritz, Analyst **133**(7), 855 (2008).
[10]G. Wu, H. Ji, K. Hansen, T. Thundat, R. Datar, R. Cote, M. F. Hagan, A. K. Chakraborty, and A. Majumdar, Proc. Natl. Acad. Sci. U.S.A. **98**(4), 1560 (2001).
[11]S. Faegh and N. Jalili, J. Micromech. Microeng. **23**(2), 025007 (2013).

[12]K. Wilson, P. Molnar, and J. Hickman, Lab Chip **7**(7), 920 (2007).
[13]M. M. Bamman, B. R. Newcomer, D. E. Larson-Meyer, R. L. Weinsier, and G. R. Hunter, Med. Sci. Sports Exercise **32**(7), 1307 (2000).
[14]R. J. Maughan, J. S. Watson, and J. Weir, J. Physiol. (London) **338**, 37 (1983).
[15]R. J. Maughan, J. S. Watson, and J. Weir, Eur. J. Appl. Physiol. **50**(3), 309 (1983).
[16]P. E. Kosnik, J. A. Faulkner, and R. G. Dennis, Tissue Eng. **7**(5), 573 (2001).
[17]L. M. Larkin, J. H. Van der Meulen, R. G. Dennis, and J. B. Kennedy, In Vitro Cell. Dev. Biol.: Anim. **42**(3–4), 75 (2006).
[18]G. G. Stoney, Proc. R. Soc. London, Ser. A **82**(553), 172 (1909).
[19]M. Das, J. Rumsey, N. Bhargava, C. Gregory, L. Riedel, J. Kang, and J. Hickman, In Vitro Cell. Dev. Biol.: Anim. **45**(7), 378 (2009).
[20]M. Das, J. W. Rumsey, N. Bhargava, M. Stancescu, and J. J. Hickman, Biomaterials **30**(29), 5392 (2009).
[21]M. Das, J. W. Rumsey, C. A. Gregory, N. Bhargava, J. F. Kang, P. Molnar, L. Riedel, X. Guo, and J. J. Hickman, Neuroscience **146**(2), 481 (2007).
[22]W. S. Rasband, *ImageJ* (U.S. National Institutes of Health, Bethesda, Maryland, 1997–2012).
[23]C. Ziegler, Anal. Bioanal. Chem. **379**(7–8), 946 (2004).
[24]V. T. Srikar and S. M. Spearing, Exp. Mech. **43**(3), 238 (2003).
[25]P. Schantz, E. Randall-Fox, W. Hutchison, A. Tyden, and P. O. Astrand, Acta Physiol. Scand. **117**(2), 219 (1983).